

# Stripe width and non-local domain walls in the two-dimensional Dipolar Frustrated Ising Ferromagnet

Alessandro Vindigni,<sup>1</sup> Niculin Saratz,<sup>1</sup> Oliver Portmann,<sup>1</sup> Danilo Pescia,<sup>1</sup> and Paolo Politi<sup>2</sup>

<sup>1</sup>*Laboratorium für Festkörperphysik, Eidgenössische Technische Hochschule Zürich, CH-8093 Zürich, Switzerland*

<sup>2</sup>*Istituto dei Sistemi Complessi, Consiglio Nazionale delle Ricerche,  
Via Madonna del Piano 10, 50019 Sesto Fiorentino, Italy*

(Dated: February 29, 2008)

We describe a novel type of magnetic domain wall which, in contrast to Bloch or Néel walls, is non-localized and, in a certain temperature range, non-monotonic. The wall appears as the mean-field solution of the two-dimensional ferromagnetic Ising model frustrated by the long-ranged dipolar interaction. We provide experimental evidence of this wall delocalization in the stripe-domain phase of perpendicularly magnetized ultrathin magnetic films. In agreement with experimental results, we find that the stripe width decreases with increasing temperature and approaches a finite value at the Curie-temperature following a power law. The same kind of wall and a similar temperature dependence of the stripe width is expected in the mean-field approximation of the two-dimensional Coulomb frustrated Ising ferromagnet.

PACS numbers: 75.60.Ch, 05.70.Fh, 64.60.Cn

*Introduction.*— Recent rigorous works [1, 2] state that the spontaneous magnetization of a two-dimensional (2d) Ising ferromagnet vanishes exactly if a dipolar coupling is present (Dipolar Frustrated Ising Ferromagnet, DFIF). Frustrating interactions on different spatial scales occur e.g. in ultrathin magnetic films where the spins point perpendicular to the film plane [1, 3, 4, 5, 6, 7, 8, 9, 10, 11, 12, 13, 14]. Several approaches indicate a striped ground state [1, 3, 6, 15, 16] with spin modulation along one in-plane direction and uniform spin alignment along the orthogonal in-plane direction. At finite temperatures, such spin “microemulsions” [17] suffer from the Landau-Peierls instability [1, 5, 9, 10, 11, 12, 13, 14] that delocalizes, in the thermodynamic limit, the stripe position, thus reducing the positional order to quasi-long range [2, 5, 9]. Notice, however, that the stripe width remains well defined at finite temperatures even in the thermodynamic limit [18], and that experiments on real systems do indeed observe the persistence of stripe order at finite temperatures [4, 7, 11, 12, 19], possibly because of domain-wall pinning [9, 20, 21]. It is thus worthwhile to study the Mean-Field (MF) behavior of a DFIF at finite temperature in the hope that some characteristics are “robust” enough to be valid beyond the MF approximation and to be observable in experiments. Competing interactions acting on different length scales are fundamental to many different chemical and physical systems [4, 22, 23, 24, 25] so that robust MF results on such a general model like the DFIF may have a wide significance.

A central question that motivated this work is the equilibrium stripe width  $h^*$  (number of lattice parameters) at finite temperatures. One result appears to be well established in 2d: The stripe width in the ground state depends exponentially on the ratio between the exchange ( $J$ ) and the dipolar ( $g$ ) energy per atom [1, 8, 9, 16, 17]. The temperature dependence, instead, is controversial. Within the MF approximation,  $h^*$  is expected to decrease with temperature, because it should reach a finite value

on the order of  $\frac{J}{g}$  at the temperature  $T_c$  of the MF transition to the paramagnetic state where the spin averages to zero at every site [8, 15]. Theoretical arguments based on sharp interfaces [26, 27, 28] predict a (stretched) exponential decrease of  $h^*(T)$  down to an atomic length scale at the transition temperature  $T_c$ . Within the spherical approximation, the modulation length of a related model (the Coulomb Frustrated Ferromagnet) “monotonically increases with temperature until it diverges at a disorder line temperature”, and this independently of the dimensionality of the system [29]. Experimental results on the temperature dependence of the stripe width are controversial as well [12, 19, 24] and in some cases experiments do not show any change of  $h^*$  with temperature [4].

In spite of its apparent simplicity, a detailed study of the stripe width of a DFIF as a function of temperature within the MF approximation has not been reported yet. Here, we fill this gap and solve the relevant MF equations for the DFIF model on a discrete lattice, finding a number of unexpected results. 1) The sharp-interface assumption gives the correct stripe width at low temperatures, but fails to reproduce the results of the full MF calculation close to the transition temperature  $T_c$ . 2) Near  $T_c$ , the temperature dependence of  $h^*$  crosses over to a power law. 3) This cross-over is accompanied by a delocalization of the wall between adjacent stripes: The profile changes from square-like at low temperatures to cosine-like at  $T_c$ . 4) At intermediate temperatures, the interface between two adjacent stripes develops a pronounced non-monotonic “shoulder” tailing down toward the center of the stripe according to a power law. The non-local walls are in striking contrast to the profile of the domain walls encountered in the Ising model without dipolar interaction [30] and also with the shape of conventional Bloch or Néel walls dividing domains in typical Heisenberg or planar ferromagnets [31]. The strength of the “shoulder” structure at intermediate temperatures depends on the relative strength of  $J$  and  $g$ , but it oc-

curs over mesoscopic scales and in a sizeable range of temperatures so that it should be observable by spatially resolved experiments which have a high enough signal-to-noise ratio. The cosine-like profile, instead, is realized sufficiently close to  $T_c$  independently of the ratio  $\frac{J}{g}$ . Here we provide experimental evidence that the spin profile of the stripes changes indeed from square-like at low temperatures to cosine-like at  $T_c$ .

*The model.*— The DFIF Hamiltonian on a discrete lattice reads  $\mathcal{H} = -\frac{J}{2} \sum_{\langle i,j \rangle}^N \sigma_i \sigma_j + \frac{g}{2} \sum_{\{i \neq j\}}^N \frac{\sigma_i \sigma_j}{|\vec{r}_{ij}|^3}$  where  $i$  and  $j$  are two-dimensional indices ( $i \equiv (i_x, i_y)$ ) with  $1 \leq i_x \leq L_x$  and  $1 \leq i_y \leq L_y$ ,  $\sigma_i = \pm 1$ ,  $\langle i, j \rangle$  means that the sum is restricted to nearest neighbors,  $\{i \neq j\}$  indicates a sum over all the different pairs in the lattice, and  $N = L_x \cdot L_y$  is the total number of spins. This system is treated in the MF approximation and the spin superstructure is assumed to be a stripe pattern (a very common pattern in real systems), *i.e.* we require the averages  $m_{(i_x, i_y)} \doteq \langle \sigma_{(i_x, i_y)} \rangle$  to be translationally invariant along the  $y$ -direction and periodic along the  $x$ -direction with a period of  $2h$ :  $m_{(i_x, i_y)} \equiv m_{i_x}$  and  $m_{i_x + \alpha h} \equiv (-1)^\alpha m_{i_x}$ , where  $\alpha \in \mathbb{Z}$ . The relevant MF quantities are thus reduced to the  $h$  independent variables  $m_{i_x}$ . To determine the equilibrium configurations, we first find the profile for given  $h$  from the self-consistent MF equations  $m_{i_x} = \tanh(\beta \sum_{j_x} V_{i_x, j_x}^h m_{j_x})$ , where  $\beta = 1/k_B T$  and  $V_{i_x, j_x}^h$  is the effective interaction matrix[32]; then we minimize the free energy per spin

$$F^h = \frac{1}{2h} \sum_{i_x=1}^h \sum_{j_x=1}^h V_{i_x, j_x}^h m_{i_x} m_{j_x} - \frac{1}{h} \beta^{-1} \sum_{i_x=1}^h \ln \left[ 2 \cosh \left( \beta \sum_{j_x=1}^h V_{i_x, j_x}^h m_{j_x} \right) \right]$$

with respect to  $h$ .

*The stripe width.*— Typically, in thin magnetic films  $J \gg g$ . We are thus interested in large ratios  $\delta \equiv J/g$ , for which we recover the value of  $h^*(T=0)$  known from Ref. [16] and the finite value  $h^*(T_c)$  known from Ref. [8].  $T_c$  and the limiting magnetization profile  $m_{i_x}(T \rightarrow T_c)$  (see Fig. 2a) are found as the maximum eigenvalue and the corresponding eigenvector of  $V_{i_x, j_x}^h$  [33].

In Fig. 1, we plot  $h^*(T)$  for  $\delta = 10$ . The polygonal appearance of the graphs is due to  $h^*$  changing only by  $\pm 1$  in a discrete model. In order to understand the low-temperature behavior of  $h^*(T)$  and the low-T plateau, we introduce a manageable “sharp-interface” two-spin model, where  $m_1 = m_h \equiv m_w$  and  $m_{i_x} \equiv m_b$  for  $i_x \neq 1, h$  (lower left inset of Fig. 1). In the limit of large  $\delta$ ,  $m_b$  is just the MF value for a ferromagnetic Ising model,  $m_b = \tanh(4\beta J m_b)$ , and  $m_w$  is the corresponding MF value for a spin adjacent to a domain wall,  $m_w = \tanh(\beta J(m_w + m_b))$ . Due to the reduced exchange energy in the argument of the tanh,  $m_w(T) \leq m_b(T)$  (see later Fig. 2a). Inserting  $m_w(T)$  and  $m_b(T)$  into the sharp-interface free energy and minimizing it with respect to  $h$ , we obtain  $h_{2\text{spin}}^*(T) = \exp(1 + A/4gm_b^2)$ , where

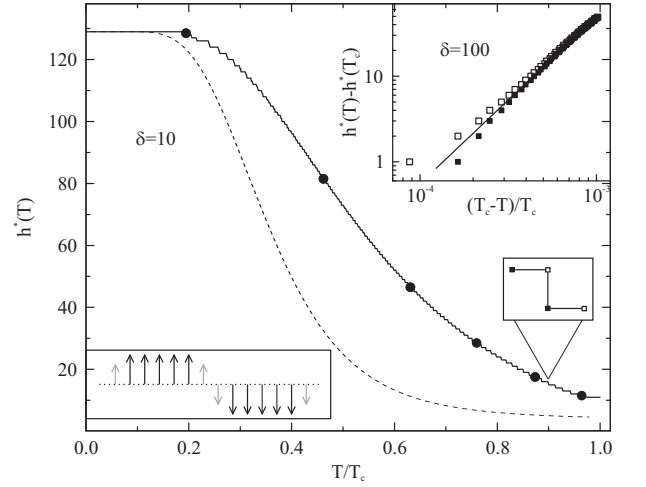


FIG. 1: Equilibrium stripe width. The solid line represents  $h^*(T)$  as a function of the reduced temperature  $T/T_c$  for  $\delta = 10$ . The dots on the line are those points for which we show spin profiles in Fig. 2a. The upper inset plots  $h^*(T) - h^*(T_c)$  versus  $(T_c - T)/T_c$  in the critical region for  $\delta = 100$ . Full (empty) dots correspond to the upper (lower) corners of the steps of the  $h^*(T)$ -curve (see sketch, lower right). A fit to the full dots is shown. The fit of the full (empty) dots gives an exponent of 2.0 (1.9). The dashed line shows  $h_{2\text{spin}}^*(T)$  calculated within the two-spin model (sharp-interface limit) for  $\delta = 10$ . The lower left inset is a cartoon visualizing the two-spin model.

$A = J(m_w^2 + m_w m_b - 4m_b^2) - k_B T \ln[(1 - m_b^2)/(1 - m_w^2)]$ . The dashed curve in Fig. 1 representing  $h_{2\text{spin}}^*(T)$  for  $\delta = 10$  reproduces the low-temperature behavior of the numerical solution but fails at higher temperatures, where it gives  $h_{2\text{spin}}^*(T_c) \approx 1$ . In the upper inset of Fig. 1, we plot  $h^*(T) - h^*(T_c)$  vs  $(T_c - T)/T_c$  for the full MF calculation close to  $T_c$  in a log-log plot, showing that the domain width behaves asymptotically according to a power law  $h^*(T) - h^*(T_c) \sim (T_c - T)^\lambda$ , with  $\lambda \approx 2$  as discussed in the figure caption. This numerical outcome seems to confirm the conjecture of Ref. [19], but is at odds with the sharp-interface limit of Refs. [26, 27, 28]. It would be interesting to review the experimental results of Ref. [12, 24] under the point of view of a power law. The argument of Ref. [19] associates the cross-over to the power-law behavior with the higher harmonics (responsible for the sharp interface at low temperatures) vanishing with increasing temperature and thus with the broadening of the spin profile to a cosine-like profile close to  $T_c$ .

*The magnetization profile.*— The spin profiles  $m_{i_x}$  at different temperatures, obtained from the transcendental MF equations, are plotted in Fig. 2a for selected temperatures (marked with dots in Fig. 1). We identify three regimes: (i) A low- $T$  regime, corresponding to the plateau in the  $h^*(T)$  curves, with a square-like profile. (ii) An intermediate  $T$  regime, corresponding to the steep descent of  $h^*(T)$ . Here, a novel feature consisting of a double-shoulder and a wall delocalization are

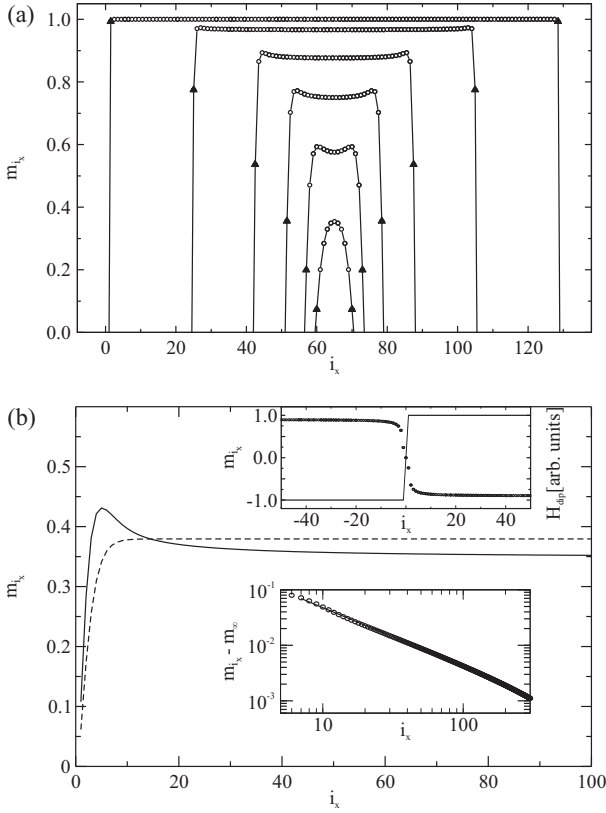


FIG. 2: (a) Spin profile within a stripe calculated for  $\delta = 10$  at different temperatures and the corresponding values of  $h^*(T)$ . The triangles locate the interface spins. (b) Spin profile for a single domain wall with  $\delta = 10$  (solid line) and  $\delta = \infty$  (“Landau” profile, dashed line), for  $T/T_C = 0.95$ . The magnetization approaches the  $m(\infty)$ -value exponentially for  $\delta = \infty$ , but it decays as  $1/i_x$  for finite  $\delta$  (lower inset). The upper inset shows the demagnetizing field (dots) originating from the dipolar interaction for a step-like spin profile (solid line).

observed. (iii) A high- $T$  regime, corresponding to the critical region, where the magnetization has indeed the cosine-like profile also expected from analytical considerations and leading to the power-law behavior of the equilibrium stripe width [19]. Notice that only within the first regime is the interface sharp and does the bulk magnetization  $m_2, \dots, m_{h-1}$  (circles) not change very much, so that the two-spin model (dashed curve in Fig. 1) is indeed justified. In order to understand the origin of the non-monotonic shoulder and the wall delocalization we have solved the MF equations for a single domain wall. In Fig. 2b we compare the profiles in the absence (dashed line) and in the presence (solid line) of the dipolar interaction. For  $\delta = \infty$  ( $g = 0$ ), the profile is of the Landau-type; it increases monotonically and attains the asymptotic value exponentially. For finite  $\delta$ , the profile is not monotonic: it has a shoulder close to the wall center and then decays to  $m(+\infty)$  as the inverse of the distance (lower inset). Both features derive from the dipolar (de-

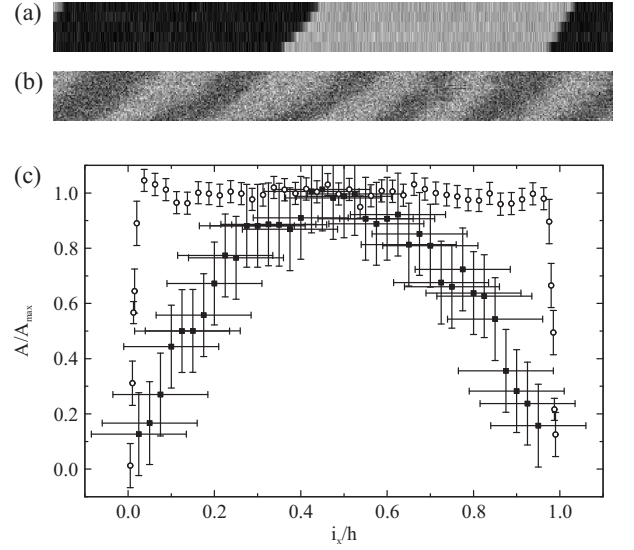


FIG. 3: (a) SEMPA [19, 34] measurement of a stripe section at low temperature (10 K). The spin polarization is encoded by a gray scale. The measured image is 4000 pixels ( $17 \mu\text{m}$ ) wide and 5 pixels (21 nm) high. For better inspection, the image has been stretched by a factor of 70 along the vertical direction. Within the spatial resolution of the experiment, this measurement corresponds to 5 scans of the same scan line, displayed as successive lines in one image. Thermal drift causes some displacement between the scan lines. (b) SEMPA measurement of a stripe section at high temperature (330 K). The measured image is 400 pixels ( $4.25 \mu\text{m}$ ) wide and 35 pixels (370 nm) high. This image is displayed in its real proportions. (c) Experimental spin profiles across one stripe at low temperature (10 K,  $h = 9 \mu\text{m}$ , empty circles) and close to the transition temperature (330 K,  $h = 430 \text{ nm}$ , black squares) as extracted from images (a) and (b) respectively. To obtain the profile, the scan lines are aligned to compensate for the thermal drift and then the aligned scan lines are averaged. To further reduce the noise level, these raw profiles are resampled by averaging a number of adjacent points. Both profiles have been normalized to the same width and amplitude. The horizontal error bars represent the spatial resolution ( $\pm 50 \text{ nm}$ ) of the experiment. It is determined from the topographic profile of a sharp edge, obtained by the same procedure from a topographic image measured with exactly the same parameters as the magnetic image 3b. For the low- $T$  profile, the horizontal error is on the order of the size of the data points. The vertical error bars are due to the statistical noise of the secondary electrons counted in SEMPA [19, 34]. Note that no traces of an in-plane component of the spin polarization can be found in simultaneously recorded images of the in-plane spin polarization. Details of the experiment will be published in a more extended review and are available on request.

magnetizing) field  $H^{\text{dip}}(i_x)$ , which is plotted for a step-like profile in the upper inset. Close to the center of the wall,  $H^{\text{dip}}(i_x)$  almost vanishes because of the compensation between the fields generated by up and down spins. There, the deviation from the Landau-type wall (dashed line) is small. The approach to the  $H^{\text{dip}}(+\infty)$

value occurs as  $1/i_x$  and depresses the spin profile below the asymptotic value for  $g = 0$ . We have also checked within a continuum model that the demagnetizing field far from the wall vanishes in the infinite-thickness limit so that the three-dimensional, monotonic and localized “Landau” wall is recovered in 3d. Thus, the formation of the non-monotonic long-ranged wall is a purely two-dimensional effect.

The square-like profile at low temperatures delocalizes into a cosine-like profile close to  $T_c$ , no matter how small the dipolar interaction is. We provide experimental evidence of this wall delocalization in Fig. 3. The spin profile was measured in SEMPAs [19] experiments on ultrathin Fe films grown epitaxially on Cu(100). These systems are magnetized perpendicularly to the film plane and show the sought-for stripe structure [34]. The two different profiles at low temperature (empty dots) and close to the stripe-paramagnetic transition temperature (full dots) point to the realization of the MF cross-over shown in Fig. 2a.

*Conclusions.*— In summary, we have shown that when dealing with “spin microemulsions” (and probably with analogous pattern-forming systems), the range of validity of the sharp-interface limit must be evaluated carefully and that important physical features, like the stripe

width, crucially depend on whether the actual interface is sharp or not. In addition, we have discovered that the “Landau”-type walls (and probably the Bloch- and Néel-type walls as well) must be modified in low-dimensional systems because the dipolar interaction produces a non-monotonic, long-range tail which is absent in 3d systems such as those considered by Landau [31]. Our study has focused on the DFIF model on a discrete lattice. However, its results appear to be relevant [35] for the Coulomb Frustrated Ising Ferromagnet [36] as well. In the Coulomb system, antiferromagnetic interactions decay as  $|\vec{r}|^{-1}$  rather than  $|\vec{r}|^{-3}$  as the dipolar interaction, but preliminary results indicate that the phenomenology (domain shrinking, power-law approach to a finite value at  $T_c$ , delocalization and presence of a shoulder in the domain wall profile) is the same. Although our work is based on the MF approximation, it produces results which appear to be realized in real pattern-forming systems, such as the power-law dependence of the stripe width [19] and the spin profile (Fig. 3c), and it might provide a reasonable starting point for more sophisticated theoretical work.

We acknowledge financial support by ETHZ and the Swiss National Science Foundation and fruitful discussions with S.A. Cannas, E. Tosatti, G.E. Santoro and Z. Nussinov.

- 
- [1] A. Giuliani, J. L. Lebowitz, and E. Lieb, Phys. Rev. B **74**, 064420 (2006).
  - [2] M. Biskup, L. Chayes, and S. A. Kivelson, Comm. Math. Phys. **274**, 217 (2007).
  - [3] C. Kooy and U. Enz, Philips Res. Repts. **15**, 7 (1960).
  - [4] M. Seul and D. Andelman, Science **267**, 476 (1995) and references therein.
  - [5] T. Garel and S. Doniach, Phys. Rev. B **26**, 325 (1982).
  - [6] Kwok-On Ng and D. Vanderbilt, Phys. Rev. B **52**, 2177 (1995).
  - [7] D. Sornette, J. Physique I (Paris) **48**, 151 (1987) and references therein.
  - [8] R. Czech and J. Villain, J. Phys. Cond. Matter **1**, 619 (1989).
  - [9] A. B. Kashuba and V. L. Pokrovsky, Phys. Rev. B **48**, 10335 (1993). Ar. Abanov, V. Kalatsky, V. L. Pokrovsky, and W. M. Saslow, Phys. Rev. B **51**, 1023 (1995).
  - [10] K. De’Bell, A. B. MacIsaac and J. P. Whitehead, Rev. Mod. Phys. **72**, 225 (2000); S. A. Cannas, D. A. Stariolo, and F. A. Tamarit, Phys. Rev. B **69**, 092409 (2004) and references therein.
  - [11] R. Allenspach and A. Bischof, Phys. Rev. Lett. **69**, 3385 (1992).
  - [12] C. Won, Y. Z. Wu, J. Choi, W. Kim, A. Scholl, A. Doran, T. Owens, J. Wu, X. F. Jin, H. W. Zhao, and Z. Q. Qiu, Phys. Rev. B **71**, 224429 (2005).
  - [13] C. B. Muratov, Phys. Rev. E **66**, 066108 (2002).
  - [14] A. D. Stoycheva and S. J. Singer, Phys. Rev. Lett. **84**, 4657 (1999).
  - [15] J. Castro, G. A. Gehring, and S. J. Robinson, J. Magn. Mater. **214**, 85 (2000).
  - [16] A. B. MacIsaac, J. P. Whitehead, M. C. Robinson, and K. De’Bell, Phys. Rev. B **51**, 16033 (1995).
  - [17] R. Jamei, S. A. Kivelson, and B. Spivak, Phys. Rev. Lett. **94**, 056805 (2005).
  - [18] B. Jancovici, Phys. Rev. Lett. **19**, 20 (1967), Eq. (8)
  - [19] O. Portmann, A. Vaterlaus, and D. Pescia, Phys. Rev. Lett. **96**, 047212 (2006) and references therein.
  - [20] In Fe films on Cu(100), the coercive field, which is a measure of the barrier for domain-wall motion, is found to be small but finite.
  - [21] S. Lemerle, J. Ferré, C. Chappert, V. Mathet, T. Giamarchi, and P. Le Doussal, Phys. Rev. Lett. **80**, 849 (1998).
  - [22] D. Andelman, F. Brochard and J.-F. Joanny, Proc. Natl. Acad. Sci. **84**, 4717 (1987).
  - [23] P. Ball, *The self-made Tapestry: Pattern formation in Nature* (Oxford University Press, Oxford, 2001).
  - [24] S. L. Keller and H. M. McConnell, Phys. Rev. Lett. **82**, 1602 (1999) and references therein.
  - [25] F. S. Bates and G. H. Fredrickson, Phys. Today **52**, 32 (1999).
  - [26] G. A. Gehring and M. Keskin, J. Phys. Condens. Matter **5**, L581 (1993), Fig. 1.
  - [27] H. M. McConnell, Annu. Rev. Phys. Chem. **42**, 171 (1991).
  - [28] A. D. Stoycheva and S. J. Singer, Phys. Rev. E **64**, 016118 (2001).
  - [29] Z. Nussinov, J. Rudnick, S. A. Kivelson, and L. N. Chayes, Phys. Rev. Lett. **83**, 472 (1999) and Z. Nussinov, ArXiv:cond-mat/0506554.
  - [30] E. Ising, Z. Phys. **31**, 253 (1925).

- [31] L. D. Landau, *Collected Papers*, edited by D. Ter Haar, pp.101-116, (1967), Gordon and Breach, New York; A. Hubert, R. Schäfer, *Magnetic Domains*, Springer, Berlin, (2000)
- [32] The effective interaction is given by  $V_{i_x, j_x}^h = J \cdot \Delta_{i_x, j_x} - g\Gamma_{i_x, j_x}$ , where  $\Delta_{i_x, j_x}$  accounts for the number and relative orientation of spins in column  $j_x$  which are nearest neighbors of a single spin in column  $i_x$ :  $\Delta_{i_x, i_x} = 2$ ,  $\Delta_{i_x, i_x \pm 1} = 1$  ( $i_x \neq 1, h$ ),  $\Delta_{1, h} = \Delta_{h, 1} = -1$ ,  $\Delta_{i_x, j_x} = 0$  otherwise.  $\Gamma_{i_x, j_x} = \sum_{\alpha} \sum_{j_y=1}^{L_y} \frac{(-1)^{\alpha}}{|(j_x - i_x + \alpha h)^2 + (j_y - 1)^2|^{3/2}}$ , where the term for  $\alpha = 0$  has to be omitted for  $i_x = j_x$ .
- [33] The MF solution  $\underline{m} \equiv (m_1, \dots, m_h)$  fulfills the condition  $|\underline{m}|^2 \leq \frac{1}{T^2} |V^h \underline{m}|^2$  and can be written in the basis of the eigenvectors  $\underline{m}_{\mu}$  of  $V^h$  with eigenvalues  $\lambda_{\mu}$  as  $\underline{m} = \sum_{\mu} a_{\mu} \underline{m}_{\mu}$ . Then  $\sum_{\mu} a_{\mu}^2 \leq \sum_{\mu} \left( \frac{\lambda_{\mu}}{T} \right)^2 a_{\mu}^2$ . For  $T > T_c = \lambda_{\max}$ , the only solution is  $a_{\mu}^2 = 0 \forall \mu$ .
- [34] O. Portmann, A. Vaterlaus, and D. Pescia, *Nature* **422**, 701 (2003).
- [35] O. Portmann and D. Pescia (unpublished).
- [36] P. Viot and G. Tarjus, *Europhys. Lett.* **44**, 423 (1998).